

Deep Reinforcement Learning for EH-Enabled Cognitive-IoT Under Jamming Attacks

Nadia Abdolkhani, Student Member, IEEE, Nada Abdel Khalek, Student Member, IEEE,
and Walaa Hamouda, Senior Member, IEEE

Abstract—In the evolving landscape of the Internet of Things (IoT), integrating cognitive radio (CR) has become a practical solution to address the challenge of spectrum scarcity, leading to the development of cognitive IoT (CIoT). However, the vulnerability of radio communications makes radio jamming attacks a key concern in CIoT networks. In this paper, we introduce a novel deep reinforcement learning (DRL) approach designed to optimize throughput and extend network lifetime of an energy-constrained CIoT system under jamming attacks. This DRL framework equips a CIoT device with the autonomy to manage energy harvesting (EH) and data transmission, while also regulating its transmit power to respect spectrum-sharing constraints. We formulate the optimization problem under various constraints, and we model the CIoT device’s interactions within the channel as a model-free Markov decision process (MDP). The MDP serves as a foundation to develop a double deep Q-network (DDQN), designed to help the CIoT agent learn the optimal communication policy to navigate challenges such as dynamic channel occupancy, jamming attacks, and channel fading while achieving its goal. Additionally, we introduce a variant of the upper confidence bound (UCB) algorithm, named UCB-IA, which enhances the CIoT network’s ability to efficiently navigate jamming attacks within the channel. The proposed DRL algorithm does not rely on prior knowledge and uses locally observable information such as channel occupancy, jamming activity, channel gain, and energy arrival to make decisions. Extensive simulations prove that our proposed DRL algorithm that utilizes the UCB-IA strategy surpasses existing benchmarks, allowing for a more adaptive, energy-efficient, and secure spectrum sharing in CIoT networks.

Index Terms—Cognitive Internet of Things, deep reinforcement learning, upper confidence bound, energy harvesting, jamming attacks.

I. Introduction

IN the midst of the rapid proliferation of Internet of Things (IoT) devices and services, IoT networks grapple with spectrum scarcity and congestion challenges. Given that IoT lacks dedicated bandwidth and shares the spectrum with various RF technologies like Bluetooth, addressing these challenges becomes imperative [1]. Cognitive radio (CR) technology has emerged as a strategic solution that allows IoT devices to efficiently share the spectrum with licensed users, or primary users (PUs), thereby improving the spectral utilization efficiency [2]. There are three main CR access approaches by which

N. Abdolkhani, N. Abdel Khalek, and W. Hamouda are with the Department of Electrical and Computer Engineering, Concordia University, Montreal, QC, H3G 1M8, Canada (e-mail: n_abdolk@ece.concordia.ca; n_abdelk@ece.concordia.ca; hamouda@ece.concordia.ca).

secondary users (SUs) or unlicensed users can access the spectrum, which are the interweave, underlay, and overlay approaches. Using the interweave approach, SUs can only access the licensed spectrum if and only the PUs are not utilizing it [3]. On the other hand, in the underlay approach both the SUs and PUs coexist provided that the SUs do not interfere with the PUs [4]. Finally, in the overlay approach, the SUs assist the PUs in exchange for spectrum access privileges [5].

To effectively share the spectrum in underlay CR, cognitive IoT (CIoT) devices have to dynamically adjust their transmission power to abide by the interference constraint set by the primary network while also aiming to maximize their throughput. Effective power control is essential, especially for energy-constrained CIoT devices, which must not only focus on maximizing their throughput but also on extending the network’s lifetime. Energy harvesting (EH) offers a solution for CIoT devices to overcome their energy constraints, allowing them to be self-sufficient and ensuring network continuity without the necessity for external sources. EH involves harnessing energy from renewable sources in the environment, such as solar, wind, and radio frequency (RF) signals. Among these sources, RF signals offer a particularly promising future due to their predictable, stable nature, and cost-effectiveness [6], [7]. In RF EH, CIoT devices can gather energy from RF signals produced by nearby devices to recharge their batteries [8]. That is, EH RF allows CIoT devices to operate completely untethered, eliminating the need for support from a wired power source or frequent battery replacements.

Although CIoT networks benefit from the opportunistic spectrum access, they are vulnerable to jamming attacks given the inherent shared and broadcast nature of radio wave propagation [9]. As indicated by [10], the ease of launching jamming attacks, thanks to the advancements in software-defined radio, underscores the urgency of securing wireless networks against both intentional and unintentional jamming. In the presence of such attacks, the jammer can disrupt communication channels by introducing continuous jamming signals or brief jamming pulses across single or multiple frequency bands, leading to a degradation in the signal-to-noise ratio (SNR) [10]. Consequently, the throughput capacity of ongoing transmissions diminishes, and in some cases, the transmission may be completely interrupted [11]. Therefore, jamming attacks pose a significant threat to CIoT transmissions, especially

under energy and spectrum sharing constraints. Hence, there is a need for robust and intelligent countermeasures that not only enhance the performance of CIoT networks but also ensure their security and prolong their lifetime.

II. Background and Motivation

A. Related Works

Game theory has been employed in the literature for anti-jamming communication strategies [12]–[15]. Jia et al. [12] explored anti-jamming channel selection strategies in dense wireless networks under the presence of jammers, framing the anti-jamming communication problem as a Stackelberg game. A multi-domain anti-jamming strategy, considering both time and power domains, was proposed in [15]. Using a Stackelberg game model, a genetic algorithm was developed to determine the optimal frequency-hopping speed and transmit powers. The Colonel Blotto anti-jamming game in [13] offers a defense strategy for slow fading IoT networks using orthogonal frequency-division multiplexing channels. This approach minimizes the worst-case jamming effect and optimizes power allocation, effectively combating jamming attacks while conserving IoT sensors' power.

In multi-user networks, Xu et al. investigated a game-theoretic anti-jamming spectrum access approach [14]. The authors develop an internal coordination-external confrontation game model and design a coordination-learning-based anti-jamming spectrum access algorithm to achieve correlated equilibrium. While game-theoretical strategies have been explored for anti-jamming communications, they often rely on impractical prerequisites such as prior knowledge of the jamming pattern and may prove ineffective when confronted with constantly evolving jamming tactics [16]. Consequently, the utilization of intelligent algorithms in anti-jamming communications is encouraged due to their increased unpredictability for jammers, as these algorithms dynamically adjust to the spectrum's state [17].

By employing reinforcement learning (RL) algorithms, jamming behaviors can be learned through a process of “trial-and-error” with the environment, even without access to specific information about the jammer. Works such as [5], [18]–[22] have addressed jamming attacks in the spectrum domain by using learning-based frequency hopping strategies. Ali et al. proposed an energy-efficient Dueling deep Q-network (DQN) for implementing an anti-jamming frequency hopping strategy in CIoT networks [18]. Shen et al. employed a convolutional double deep Q-network (DDQN) for smart channel selection to counter jamming attacks [19]. Aref et al. proposed a convolutional DDQN framework to address interference and jamming in wideband spectrums, focusing on reducing computational complexity [20].

To simulate the communication environment of an overlay CR network under indiscriminate jamming attacks, Han et al. utilized a generative adversarial network (GAN) [5]. Subsequently, a soft actor-critic deep

reinforcement learning (DRL) approach, incorporating convolutional layers, was used to determine the optimal spectrum access policy within the simulated environment. Zhou et al. tackled the issue of anti-jamming by using a collaborative multi-agent reinforcement learning (MARL) approach based on Q-learning for channel selection under intelligent dynamic jamming [21]. Bi et al. introduced a frequency hopping strategy for multi-user CR networks that utilizes a DDQN framework [22]. The base station takes charge of training the DDQN to identify the most effective channel selection strategy, which is subsequently deployed to the CR users post-training.

Works such as [23]–[25] have focused attention towards refining anti-jamming communication strategies that encompass not only frequency selection but also sub-band selection within each frequency. In [23], a convolutional DDQN was designed for anti-jamming communications within a heterogeneous wideband spectrum. This framework determines both the selection of sub-bands for access and the choice of channels within those sub-bands. Employing multitask transfer learning, the authors accelerate training by treating each sub-band as a distinct task. Li et al. introduced a hierarchical DRL algorithm [24]. This algorithm utilizes two convolutional DQNs, one for determining the frequency band and another for selecting the specific frequency within the chosen band, prioritizing frequencies with the lowest likelihood of being jammed. Liu et al. introduced an anti-jamming approach for both the time and frequency domains in cellular CR networks [25]. The approach utilizes a convolutional DQN with a long short-term memory (LSTM) layer and enables the CR transmitter to decide on transmission timing in the time domain and conduct joint channel-bandwidth selection in the frequency domain.

The above approaches to countering jamming attacks relied on the assumption that multiple channels are available and jammers can simultaneously target all channels. As a result, SUs may select channels less likely to be jammed or switch to an alternative channel upon encountering jamming. However, there are scenarios where SUs are configured to opportunistically transmit data on a specific channel, such as when permitted by the licensed channel holder. Therefore, power control approaches have been explored in wireless communication to counter jamming attacks. Notably, power control schemes in [26], [27] involve assessing channel conditions and adapting transmit power to counteract jamming. Geng et al. developed a dynamic anti-jamming model using Q-learning to determine the optimal anti-jamming power, where users lack knowledge of the game model [26]. Despite being employed for power control, Q-learning exhibits extended convergence times to achieve the optimal strategy when faced with a considerable number of states, and it may occasionally fail to converge [27].

Deep reinforcement learning (DRL), which combines both RL and deep learning (DL), has been utilized to overcome the challenges of Q-learning. Nguyen et al. introduced a method based on a DDQN to acquire

an effective communication policy, encompassing channel access and transmission power adjustments to address various jamming scenarios [28]. Similarly, Xu et al. use a transformer encoder-based DDQN for channel and transmit power selection by a secondary transmitter under the presence of a jammer [11]. Ali et al. used clear channel assessment data to train a DDQN to learn an effective anti-jamming strategy for a CR agent that dynamically switches channels and selects the appropriate transmit power [29]. Aref et al. proposed a multitask DQN architecture for multi-agent environments to maintain the required quality of service (QoS) by adjusting the transmit power and frequency hopping in a wideband spectrum [30]. Chen et al. proposed a convolutional DQN for power control in CIoT networks under the presence of a jammer and tested the effectiveness of their approach in realistic scenarios under hardware constraints [27].

B. Motivation and Contributions

Liu et al. explored a power control strategy to mitigate jamming attacks in CR networks [31]. However, the proposed cooperative mechanism may not suit the dynamic nature of CIoT networks, where users frequently join and leave on an ad-hoc basis, and assumes a unified objective among SUs which may not hold in practice. To date, only a handful of studies, namely [18], [27], have directly investigated anti-jamming approaches specifically tailored for CIoT networks, pointing to a significant research gap in this area. Ali et al. introduced a DRL algorithm with an emphasis on energy efficiency, aiming to implement a system architecture that conserves energy [18]. Nonetheless, we believe that focusing solely on energy-efficient DRL algorithms may not adequately account for the broader spectrum of energy constraints, particularly in scenarios involving battery-operated CIoT devices. Furthermore, the strategy in [27] that increases CIoT device transmit power to counteract jammers, presents substantial challenges in energy-limited settings. Additionally, such an approach to power control is particularly challenging in underlay CR environments, where SUs and PUs share the spectrum. Studies such as [18], [27], [32] have overlooked spectrum-sharing scenarios in CR networks. Moreover, [27], [32] overlook the impact of channel fading effects, further underscoring the need for a comprehensive solution.

To the best of the authors' knowledge, no previous research has considered designing an intelligent algorithm that aims to maximize the CIoT network's throughput under interference limits, energy constraints, and jamming attacks. The main contributions of the paper are summarized as follows:

- We introduce a novel strategy for a battery-powered CIoT transmitter, enabling autonomous decision-making to enhance long-term network throughput within spectrum-sharing limits, mitigate jamming interference, and extend network life. Our method uniquely positions the CIoT transmitter to counter

jamming attacks directly in the same channel. Additionally, we evaluate the influence of small-scale fading and implement an effective EH model, allowing the CIoT transmitter to exclusively harvest energy from active RF transmissions without dedicating infrastructure for charging.

- We formulate the throughput optimization problem for the CIoT transmitter while taking into account factors such as channel occupancy, jamming attacks, channel gain, energy arrival, battery limits, and interference constraints. This approach directs the power control and transmission decisions in the CIoT network, modelled as a model-free Markov decision process (MDP).
- We develop a novel DRL algorithm to learn the optimal transmission strategy that maximizes throughput without prior knowledge about the channel or jamming patterns. Our algorithm uses a DDQN designed to enable faster convergence and enhance the algorithm's energy efficiency. Additionally, we introduce an innovative upper confidence bound (UCB) strategy, named UCB interference-aware (UCB-IA), meticulously designed to efficiently mitigate jamming interference and optimize the decision-making framework within the CIoT environment.
- We offer an analysis of convergence and performance of the proposed DRL algorithm that is benchmarked against alternative methodologies found in existing literature across various test scenarios. For performance evaluation, we utilize metrics such as average sum rate, average achievable reward, and jammer interference ratio. Simulations show that under the presence of jamming attacks, the proposed learning algorithm can dynamically choose between data transmission and EH and perform power control to find the optimal solution for the network.

The rest of the paper is organized as follows. Section II provides the related work. Section III describes the system model, Section IV showcases the optimization problem formulation, Section V presents the proposed DRL-driven throughput optimization under malicious jamming attacks, Section VI presents the simulation model and comprehensive analysis of the paper's results, and finally, we conclude the paper in Section VII. To enhance clarity, the notations used in this paper are clearly outlined in Table I.

III. System Model

A. Cognitive IoT Network

Consider the underlay CIoT network depicted in Fig. 1 with a CIoT transmitter-receiver (Tx-Rx) pair, where the Tx is equipped with a rechargeable battery and is capable of RF energy harvesting (EH). The CIoT network shares the dedicated spectrum with the primary network, which consists of a primary Tx-Rx pair. The CIoT Tx possesses the capability to autonomously and dynamically regulate its transmit power P_s^t . The CIoT system operates in a

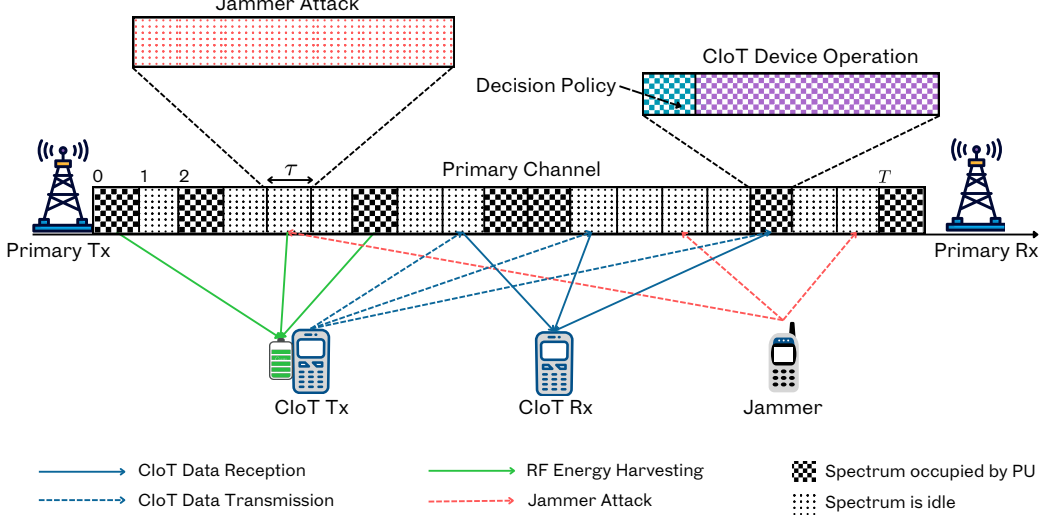


Fig. 1. System Model

time-slotted manner, with T time slots each of duration τ seconds. For the CIoT Tx, every time slot t encompasses two distinct phases: the decision-making phase and the operation phase. In the decision-making phase, the CIoT device chooses either to transmit data or to harvest energy, following a specific policy. The decision made by the CIoT Tx d_t is set to 0 when transmitting messages and to 1 when harvesting energy. Consequently,

$$d_t = \begin{cases} 0 & \text{Data transmission mode in time slot } t, \\ 1 & \text{Energy harvesting mode in time slot } t. \end{cases} \quad (1)$$

The operation phase involves the CIoT device carrying out the chosen decision d_t . We assume the number of slots used by the PU Tx is L where $1 < L < T$ and the PU Tx can consistently transmit at a power level of P_p^t at any slot.

In underlay CR, the CIoT Tx can use the same time slot as the PU Tx as long as it adheres to the interference threshold I_{th} . Therefore, the CIoT device needs to decide on its transmission power P_s^t such that it adheres to the interference constraint given as

$$P_s^t g_{sp}^t \leq I_{th}, \quad (2)$$

where g_{sp}^t is the channel power gain between the CIoT Tx and PU Rx. The PU status indicator is defined as

$$\omega_p^t = \begin{cases} 1 & \text{if the PU Tx is using time slot } t, \\ 0 & \text{otherwise.} \end{cases} \quad (3)$$

The power gains of the channel between the CIoT Tx-Rx pair is g_{ss}^t , the PU Tx and the CIoT Rx is g_{ps}^t , and the CIoT Tx and the PU Rx is g_{sp}^t , are characterized as Rayleigh fading channels that are independently and identically distributed (i.i.d.). It is assumed that these channel power gains remain constant within a time slot, but may vary independently of one time slot to another.

B. Jamming Model

We consider a jammer that launches jamming attacks on the CIoT network, as shown in Fig. 1. The goal of the jammer is to make the shared spectrum ‘‘appear’’ busy and prevent CIoT Tx from accessing it and potentially depleting the CIoT device’s battery. We consider that the jammer can only target the CIoT transmissions. This could be attributed to the potential severe penalties faced by attackers upon identification by PUs, or the inability to approach PUs. Moreover, in practice, methods such as cyclostationary detection or matched filter detection can be used by the jammers to differentiate between the PUs and CIoT transmissions. Therefore, at the beginning of each time slot, the jammer determines whether the PU is active or not before launching the jamming attack. Should a jammer initiate an attack, it will attack for the duration of the entire time slot [33]. The jammer launches a jamming attack with power P_j^t . The CIoT Tx has no prior information about which time slots will be subjected to jamming attacks.

Attackers tend to favor a random jamming approach, as it enables intermittent periods of inactivity [33]. This strategy not only prolongs the jammer’s lifetime but also decreases the chance of its detection. Therefore, we consider the scenario of intermittent jamming, where the jammer randomly toggles between periods of uniformly distributed jamming and rest. That is, the jammer engages in attacks for a duration of $\zeta \sim U(0, \zeta_{\max})$ slots, followed by a period of rest lasting $T - \zeta$ slots, where ζ_{\max} denotes the maximum number of time slots that the jammer is capable of sustaining jamming attacks. Therefore, the probability of launching an attack is $U(0, \zeta_{\max})/T$. By incorporating randomness into the jammer’s actions, the jamming behavior becomes less predictable for the CIoT Tx. In this paper, the impact of one jammer launching attacks is analogous to multiple coordinated jammers tar-

TABLE I
Notations

Notation	Definition
T	Number of time slots
t	Time slot number
τ	Duration of each time slot
B_{max}	Battery capacity of CIoT Tx
B_t	Battery level at time slot t
L	Number of PU transmission slots
ζ	Number of slots the jammer attacks
ζ_{max}	Maximum number of slots that jammer targets
P_p^t	PU transmit power in time slot t
P_s^t	CIoT Tx transmit power in time slot t
P_j^t	Transmit power of the jammer in time slot t
ω_p^t	PU status indicator in time slot t
ω_j^t	Jammer status indicator in time slot t
I_{th}	Interference threshold
d_t	CIoT device's decision to transmit/harvest
R^t	Achievable rate of the CIoT Tx in time slot t
k	Number of slots used by the CIoT Tx
g_{sp}^t	Channel power gain between the CIoT Tx and PU Rx
g_{ss}^t	Channel power gain for the CIoT Tx-Rx pair
g_{ps}^t	Channel power gain for the PU Tx and CIoT Rx
σ^2	Channel noise variance
e_t	Energy harvested in time slot t
E_{max}	Maximum possible energy to be harvested
\mathcal{S}	State space
\mathcal{A}	Action space
\mathcal{P}	Set of state transition probabilities
\mathcal{R}	Set of possible rewards
s_t	State of the environment at time slot t
a_t	Action taken by the CIoT agent at time slot t
r_t	CIoT agent's reward at time slot t
γ	Discount factor
θ	Parameters of DDQN
θ'	Parameters of Target DDQN
α	Leakiness parameter
κ	Update rate of Target DDQN
\mathcal{L}	Training loss function
\mathcal{M}	Experience replay memory
m	Memory size
η	Learning rate
\hat{r}_a	Empirical mean reward of action a
C_a	Number of times action a is chosen
U_a	Actual expected reward of action a
$\hat{\lambda}_a$	Empirical mean jammer interference of action a
\bar{U}_a	Expected jammer interference of action a
c'	UCB adjustment term

getting specific time slots for their attacks. This allows our system to be scalable to incorporate several coordinated jammers, with each one executing a jamming attack in individual time slots.

The CIoT agent determines the jammer's status indicator at the beginning of each time slot using broadband sensing capabilities [33]. The jammer's status indicator, which reflects whether the jammer is launching a jamming attack in a time slot t is defined as follows

$$\omega_j^t = \begin{cases} 0 & \text{Jammer is launching an attack at time slot } t, \\ 1 & \text{otherwise,} \end{cases} \quad (4)$$

where $\omega_j^t = 0$ indicates that the CIoT agent detects the presence of a jamming attack, following the probability $U(0, \zeta_{max})/T$, and $\omega_j^t = 1$ indicates that the CIoT agent does not detect a jamming attack, with a probability of $1 - U(0, \zeta_{max})/T$.

C. Energy Harvesting Model

The CIoT transmitter is capable of charging its finite battery, denoted by B_{max} , through RF EH¹. Initially, the harvested energy is set to zero. It is assumed that the amount of energy collected in each time slot, e_t , follows a uniform distribution ranging from 0 to E_{max} , where $e_t \sim U(0, E_{max})$. However, the maximum possible energy to be harvested E_{max} is affected by the RF signals, which are influenced by the activity of both the jammer and the PU Tx within each time slot. Thus, the value of E_{max} varies depending on the following

$$E_{max} = \begin{cases} P_p^t & \text{if } \omega_p^t = 1, \text{ PU transmitting,} \\ P_j^t & \text{if } \omega_j^t = 0, \text{ jammer is attacking,} \\ P_p^t + P_j^t & \text{if } \omega_p^t = 1 \text{ and } \omega_j^t = 0. \end{cases} \quad (5)$$

The energy collected at any given time slot is kept in the battery and is solely used for operation in future time slots. However, due to constraints in the hardware, the CIoT Tx is unable to perform RF EH and access the spectrum opportunistically at the same time. It is important to highlight that the energy harvesting process does not lead to any additional energy consumption for PUs or other devices [34].

The initial battery level of the CIoT Tx is denoted as B_0 , with B_t representing the energy available in the battery at the t -th time slot. Following the approach in [35], we assume the battery to be ideal, meaning there are no losses of energy during its storage or retrieval. For the CIoT Tx, energy consumption is exclusively due to data transmission. Moreover, any harvested energy that exceeds the battery's maximum capacity is deemed to be discarded. Additionally, the concept of normalized time slots is used, which permits treating the terms "energy" and "power" as synonymous [35]. At any given time slot t , the selected transmission power P_s^t by the CIoT Tx must not exceed the battery's total energy, B_t . That is,

$$0 \leq (1 - d_t)P_s^t \tau \leq B_t, \quad (6)$$

where τ represents the duration of each time slot. The increase or decrease in the battery's energy level is determined by the CIoT device's decision d_t to harvest energy/transmit data at a time slot t . In the subsequent time slot, $t + 1$, the amount of energy available is updated based on d_t . Therefore, the battery update is as follows

$$B_{t+1} = \min\{B_t + d_t e_t - (1 - d_t)P_s^t \tau, B_{max}\}. \quad (7)$$

Consequently, the total energy consumed by the CIoT device cannot exceed the total energy collected in the battery. That is,

$$\sum_{t=1}^k P_s^t \tau \leq B_0 + \sum_{t=0}^{k-1} e_t, \quad \forall k. \quad (8)$$

where k represents the total number of time slots in which the CIoT device decides to transmit.

¹The implementation of circuits responsible for the process of RF EH is beyond the scope of this paper.

D. Transmission Model

The CIoT Tx is tasked with setting its transmit power P_s^t such that it maximizes its sum rate under jamming attacks and avoids interfering with the primary network. During an idle t -th time slot, the achievable sum rate by the CIoT Tx is

$$R_0^t = \log_2 \left(1 + \frac{P_s^t g_{ss}^t}{\sigma^2} \right), \quad (9)$$

where σ^2 denotes the variance of the channel noise. Should the PU Tx occupy the channel during the t -th time slot, the CIoT Tx's achievable sum rate will be reduced due to PU interference, as described by

$$R_1^t = \log_2 \left(1 + \frac{P_s^t g_{ss}^t}{P_p^t g_{ps}^t + \sigma^2} \right). \quad (10)$$

Hence, the achievable sum rate for the CIoT Tx during a time slot t can be expressed as

$$R^t = \omega_j^t (1 - d_t) [(1 - \omega_p^t) R_0^t + \omega_p^t R_1^t]. \quad (11)$$

According to (11), if the jammer is launching an attack at time slot t , i.e., $\omega_j^t = 0$, then the achievable sum rate R_t of the CIoT Tx effectively drops to zero.

IV. Optimization Problem Formulation

In this section, we aim to define the optimization problem, to develop a dynamic algorithm that maximizes the total sum rate of the CIoT network. This algorithm will address challenges such as jamming attacks, channel fading, interference, and energy constraints. The CIoT device needs to learn how to optimize both its transmission power P_s^t and decision d_t to maximize the throughput of the network. That is, the CIoT device must strategically choose between transmitting data, which consumes battery and may be affected by jamming, or harvesting energy, sacrificing immediate transmission opportunities. Therefore, the optimization problem can be formulated as follows

$$\max_{P_s^t} \sum_{t=1}^T \omega_j^t (1 - d_t) [(1 - \omega_p^t) R_0^t + \omega_p^t R_1^t], \quad (12a)$$

$$\text{s.t. } \sum_{t=1}^k P_s^t \tau \leq B_0 + \sum_{t=0}^{k-1} e_t, \quad \forall k, \quad (12b)$$

$$0 \leq (1 - d_t) P_s^t \tau \leq B_t, \quad d_t \in I \triangleq \{0, 1\}, \quad (12c)$$

$$d_t = 1, \quad \forall \omega_j^t = 0, \quad (12d)$$

$$\omega_p^t g_{sp}^t P_s^t \leq I_{th}^t, \quad \omega_p^t \in \Omega \triangleq \{0, 1\}. \quad (12e)$$

Constraint (12b) ensures that the transmission power P_s^t of the CIoT device remains within the bounds set by the initial battery level B_0 and the energy harvested over all the time slots within the period. Constraint (12c) requires that the CIoT device's transmission power does not exceed the current battery level B_t in any specific time slot t . Constraint (12d) protects against the use of time slots when the jammer is active. Moreover, (12e)

dictates that the CIoT Tx complies with the interference threshold I_{th} to avoid causing interference to the PU during each time slot t . In the subsequent discussion, we introduce a solution for the optimization problem presented in (12a) by employing a model-free Markov Decision Process (MDP).

A. The Model-Free Markov Decision Process (MDP)

The process of learning the optimal strategy that maximizes the sum rate of the CIoT network can be formulated as an MDP. The MDP is represented by the tuple $(\mathcal{S}, \mathcal{A}, \mathcal{P}, \mathcal{R}, T)$, where \mathcal{S} signifies the set of CIoT environment states, \mathcal{A} represents the set of possible actions by the CIoT agent², \mathcal{P} represents the set of state transition probabilities, \mathcal{R} includes the rewards for specific state-action combinations, and T indicates the time step. In practical CR contexts, it is notably difficult to accurately determine the probability density functions of energy and channel fading [36]. Moreover, under jamming attacks, calculating the transition probabilities necessitates having full and accurate knowledge of the jamming pattern. Given that the jammer aims to disrupt the transmissions of the CIoT network and will therefore not reveal their information, obtaining the state transition probabilities proves to be impractical. Therefore, as a solution, a model-free MDP approach is utilized, and deep reinforcement learning (DRL) is employed to infer \mathcal{R} based on \mathcal{S} and \mathcal{A} , in the absence of \mathcal{P} . Consequently, the CIoT device is designed to deduce a policy $\pi : \mathcal{S} \rightarrow \mathcal{A}$ through ongoing interactions with the environment and learning from them the actions that yield the most cumulative reward. This leads to a revised model-free MDP: $(\mathcal{S}, \mathcal{A}, \mathcal{R}, T)$. The elements of this MDP tuple are detailed below.

State Space \mathcal{S} : Within each time slot, the CIoT device, acting as a learning entity, assesses the state of the unknown environment (channel) for its decision-making process. The state space comprises all possible states across the T time slots. For any given environment state s_t , the CIoT agent must consider several factors: the current level of battery B_t , the energy harvested in the preceding time slot e_{t-1} , the presence of a PU Tx, the presence of jamming attacks, and the channel power gains denoted as $g_{ps}^t, g_{sp}^t, g_{ss}^t$. Hence, the CIoT environment's state at the t -th time slot encompasses these elements as follows

$$s_t = \{B_t, e_{t-1}, \omega_p^t, \omega_j^t, g_{ps}^t, g_{sp}^t, g_{ss}^t\}. \quad (13)$$

Action Space \mathcal{A} : The action space encompasses every possible action the CIoT agent is capable of performing. For optimizing throughput, it is appropriate to consider both the decision d_t and the transmit power P_s^t as integral elements of the action. Based on the environment state s_t , the CIoT agent must choose either to transmit data ($d_t = 0$) or to harvest energy ($d_t = 1$), and set its transmission

²We use CIoT agent/device to refer to the transmitter within the network under study.

power P_s^t appropriately. Thus, the CIoT agent's action at time slot t is defined as

$$a_t = [d_t, P_s^t], \text{ where } d_t \in I \triangleq \{0, 1\}, \text{ and } P_s^t \in P. \quad (14)$$

P is the set of possible transmission powers by the CIoT agent.

Reward \mathcal{R} : The CIoT agent evaluates the effectiveness of its chosen actions through the rewards received, using this feedback to refine its decision-making strategy. As such, the reward is defined by the data transmission rate achieved by the CIoT Tx, under the condition that it adheres to the constraints specified in (12). Choosing to harvest energy results in a reward of 0. Should the CIoT Tx engage in an action a_t that breaches the constraints outlined in (12), it incurs a negative reward as a form of penalty. Thus, the reward r_t for the CIoT agent in each time slot t is determined as follows

$$r_t = \begin{cases} R_0^t & d_t = 0, \omega_p^t = 0, \omega_j^t = 1, 0 \leq P_s^t \tau \leq B_t, \\ R_1^t & d_t = 0, \omega_p^t = 1, \omega_j^t = 1, 0 \leq P_s^t \tau \leq B_t, P_s^t g_{sp}^t \leq I_{th}, \\ 0 & d_t = 1, P_s^t \tau > B_t, \\ -\phi & \text{others.} \end{cases} \quad (15)$$

Time Step T : The transition from a current time slot t to the following slot $t+1$ constitutes a discrete time step. In this framework, we analyze all possible state-action pairs within the duration of T time slots, iterating through these pairs systematically for each time slot increment.

V. DRL-Driven Throughput Optimization Under Malicious Jamming

In the specified model-free MDP, the CIoT agent faces the challenge of assessing the value of state-action pairs without prior knowledge of \mathcal{P} . However, through reinforcement learning (RL), the CIoT agent can approximate the state-value function and learn a policy π that guides action selection a_t per the current CIoT environment state s_t . The aim is to maximize the reward (sum rate) given by utilizing a policy π . This involves navigating challenges like malicious jamming while accommodating considerations for spectrum sharing, energy limitations, the variability of energy arrival, and channel fading conditions.

A policy π is a function that assigns probabilities to taking action a when in state s , mapping each state-action pair to the probability $\pi(s, a)$ of selecting action $(a \in \mathcal{A})$ in state $s \in \mathcal{S}$. For the model-free MDP, we can define the expected value of the state-action value function, also known as the Q-function or Bellman equation, as

$$Q^\pi(s, a) = \mathbb{E}[r_t + \gamma Q^\pi(s_{t+1}, a_{t+1}) | s_t = s, a_t = a], \quad (16)$$

where r_t represents the immediate reward for taking action a_t in state s_t . The term $\gamma Q^\pi(s_{t+1}, a_{t+1})$ reflects the discounted expectation of future rewards, with γ , a discount factor ranging between 0 and 1, indicating the relative significance of future rewards compared to immediate ones. Higher γ values prioritize long-term rewards more heavily. The objective for the CIoT agent

is to identify the optimal action a_t that maximizes the Q-value at each time slot t , meaning

$$a^* = \arg \max_{a \in \mathcal{A}} \{Q^\pi(s, a)\}. \quad (17)$$

Through the Q-learning algorithm, the CIoT agent determines the Q-value at every step and records it in a Q-table to identify the best solution. The most basic method for updating the action-value function is described as [37]

$$Q^\pi(s, a) = Q^\pi(s, a) + \eta \left[r_{t+1} + \gamma \max_a Q^\pi(s_{t+1}, a) - Q^\pi(s, a) \right], \quad (18)$$

where $\eta \in [0, 1]$ represents the learning rate. However, Q-learning may encounter slow convergence rates in finding the optimal actions for problem resolution [32]. Therefore, we explore deep Q-learning, integrating principles from both RL and deep learning, to estimate the Q-value function through the use of a deep neural network, also known as a double deep Q-network (DDQN). This approach aims to enhance the approximation of the Q-value function for more efficient training.

Fig. 2 provides a detailed view of the employed DRL algorithm, including our proposed UCB-IA exploration strategy, which will be discussed in the next subsections.

A. The proposed DDQN-Driven DRL Approach

In this subsection, we present our DDQN architecture, designed to determine the best policy for enhancing transmission efficiency within the CIoT network under malicious jamming attacks. Our DDQN aims to predict the total expected reward (Q-value) for every possible action a_t within a specific state s_t . Essentially, this involves adjusting the DDQN's parameters θ iteratively such that

$$Q^\pi(s, a; \theta) \approx Q^\pi(s, a). \quad (19)$$

The parameters of the DDQN, $\theta = \{W^{(i)}, b^{(i)}\}$, for the layers $i = \{1, \dots, 4\}$, signify the network's weights and biases. The DDQN employs a fully connected neural network architecture. Its input layer features j neurons that match the state space \mathcal{S} dimensionality. Additionally, the neural network includes two hidden layers with h_1 and h_2 neurons, respectively. The output layer consists of z neurons.

To promote faster convergence of the DDQN and enhance the stability of the training process, we utilize a weight initialization method called Kaiming (He) initialization [38]. This technique initializes the DDQN's weights by drawing from a Gaussian distribution $\mathcal{N}(0, \frac{2}{\nu_i})$, where ν_i denotes the count of input neurons for each layer i . To introduce non-linearity into the neural network architecture, we consider a rectified linear unit (ReLU) function. The basic ReLU activation function is expressed as $f(x) = \max(0, x)$, offering computational advantages over other activation functions such as sigmoid or hyperbolic tangent (\tanh). This is because it implements

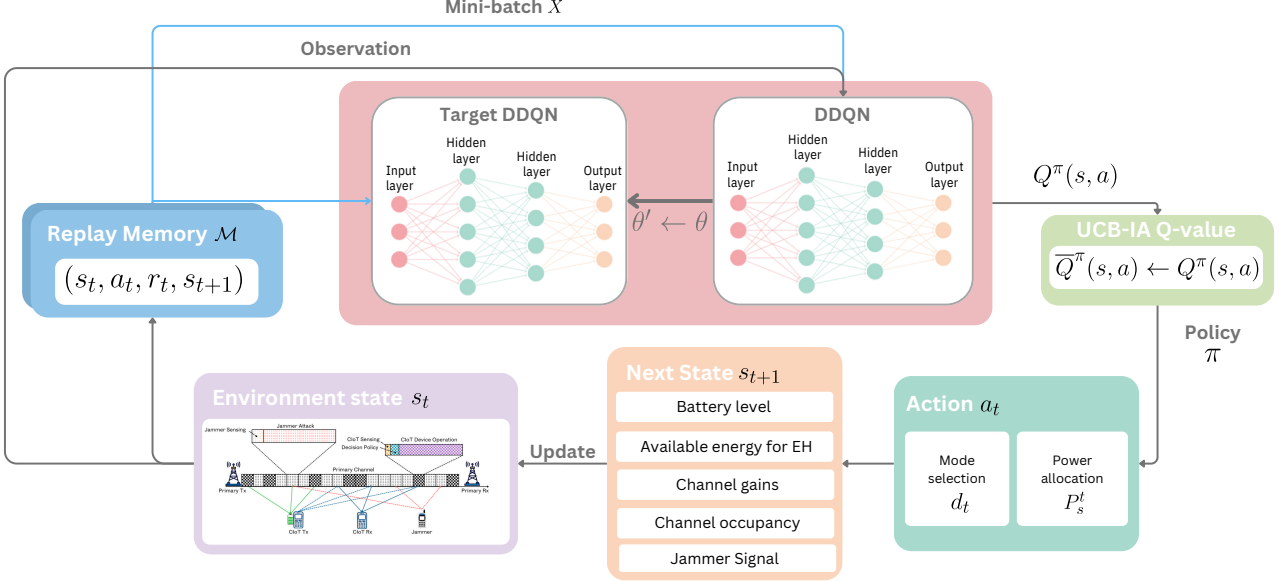


Fig. 2. The proposed DRL algorithm featuring the UCB-IA action exploration strategy.

a simple threshold at zero, significantly accelerating the training process. However, the ReLU function faces the issue of "dying ReLU" (neurons that cease to activate). To overcome this, we employ a leaky ReLU function to ensure active participation of all neurons in the learning process, which in turn facilitates quicker convergence and enhances the learning dynamics. The leaky ReLU activation function is defined as

$$f(x) = \begin{cases} x, & \text{if } x \geq 0, \\ \alpha x, & \text{if } x < 0, \end{cases} \quad (20)$$

where $\alpha \in \{0, 1\}$ represents the "slope" parameter that controls the degree of "leakiness" in the ReLU function.

To enhance the training process of the CIoT agent and ensure data efficiency, we utilize empirical replay. This involves using a memory buffer \mathcal{M} of capacity m to store previous experiences in the form of tuples (s_t, a_t, r_t, s_{t+1}) . Once the memory reaches capacity, mini-batches of experiences are randomly sampled from the data set of state-action pairs and employed in the training process to update the DDQN's parameters. By adopting this method, we can effectively eliminate temporal correlations in the training data, significantly lowering the risk of instability during the training phase [39].

Deep reinforcement learning (DRL) is known to be unstable or even diverge since it uses a non-linear deep neural network for Q-function approximation. Several factors contribute to this instability. Minor adjustments to the Q-function can drastically alter the policy, affecting data distribution. Additionally, interdependence between action-values and target values derived from maximizing Q^π over all possible actions in the next state worsens instability. Therefore, to overcome this challenge, we utilize a Target DDQN during training. The Target DDQN

is used to compute the target optimal Q-function as

$$Y = r_t + \gamma \max_{a \in \mathcal{A}} Q^\pi(s_{t+1}, a_{t+1}; \theta'), \quad (21)$$

where θ' are the Target DDQN's parameters. At the beginning of training, the Target DDQN is a mirror of the DDQN, i.e., $\theta' = \theta$. With the progression of training, the Target DDQN's parameters are updated at a slower rate than those of the DDQN, covering several training steps. The frequency of updates to the Target DDQN is denoted by κ .

To update the DDQN's parameters, we utilize the mean squared error (MSE) loss $\mathcal{L}(\cdot)$ during training to quantify the deviation between the estimated Q-values and the target Q-values across a mini-batch of state-action pairs (s, a) .

$$\mathcal{L}(\theta) = \mathbb{E} \left[\left[Y - Q^\pi(s, a; \theta) \right]^2 \right]. \quad (22)$$

During the training phase, the objective is to minimize the loss described in (22) across a mini-batch of state-action pairs. This entails

$$\hat{\theta} = \arg \min_{\theta} \mathcal{L}(\theta; s, a). \quad (23)$$

The backpropagation algorithm [40] is effective in computing $\nabla_{\theta} \mathcal{L}(\theta; s, a)$, the gradient of the loss with respect to the DDQN's parameters given the state-action pairs. Once $\nabla_{\theta} \mathcal{L}(\theta; s, a)$ is obtained, stochastic gradient descent (SGD) [36] can then be employed to update the DDQN's parameters accordingly as

$$\theta = \theta - \eta \nabla_{\theta} \mathcal{L}(\theta; s, a),$$

where $\theta = \{W^{(i)}, b^{(i)}\}$,
for $i = \{1, \dots, 4\}$. (24)

$\eta \in \{0, 1\}$ is the learning rate that determines the update rate in each iteration of SGD.

In this paper, we utilize an advanced SGD-based parameter update technique known as adaptive moment estimation (Adam) due to its faster computation time [41], [42]. Additionally, we incorporate a carefully designed learning rate scheduler. Initially, it sets a learning rate to ensure stable learning in the early phases. As training progresses, the scheduler dynamically adjusts the learning rate based on factors such as model performance and a specified patience period. This approach facilitates efficient convergence and enhances overall performance. The block diagram of the DDQN approach, thoroughly explained in this subsection, is presented in Fig. 2.

B. UCB-IA: Interference-Aware Action Exploration Strategy

As it is well known in the literature, there is a trade-off between the exploration of new actions in the action space (i.e. learning their mean reward) and the exploitation of known actions (i.e. achieving the highest empirical rewards). If the expected rewards of actions were known, the optimal policy would always choose the action that offers the highest expected reward. For the CIoT agent to explore the environment, discover optimal strategies, and balance the exploitation-exploration tradeoff we employ the principles of the upper confidence bound (UCB) algorithm.

The classical UCB algorithm adjusts the Q-values based on $\bar{Q}^\pi(s, a) = Q^\pi(s, a) + U_a^t$, where U_a^t is the actual expected reward calculated as $U_a^t = \hat{r}_a^t + \sqrt{\frac{c' \ln t}{C_a^t}}$, where c' is a hyperparameter of the UCB algorithm. The actual expected reward U_a^t is a combination of the expected reward \hat{r}_a^t and an adjustment term which depends on the time period number, i.e., frame number * $T + t$, and the number of times action a has been chosen C_a^t . If action a has been chosen C_a^t times by the end of time slot t (i.e., from 0 to t), then $\hat{r}_a^t = (\sum_{i=1}^{C_a^t} r_{a,i}^t) / C_a^t$, where $r_{a,i}^t$ is the reward of action a in the i -th time it was chosen. Then, the action returned by the UCB algorithm is used in the DDQN training and the action count C_a^t and expected reward \hat{r}_a^t are updated accordingly.

In this work, we propose a novel variant of the UCB algorithm called Interference-Aware UCB (UCB-IA), which is illustrated in Algorithm 1. The proposed UCB-IA exploration-exploitation strategy not only takes the expected reward \hat{r}_a^t to update the Q-value, but also takes the actual expected jammer interference $\hat{\lambda}_a^t$. This addition allows the agent to refine its performance by identifying actions that experience jammer interference in any state s_t , thereby adjusting the Q-values to achieve a higher reward rate while minimizing jammer interference. Therefore, under the UCB-IA strategy, the actual expected reward \bar{U}_a^t is defined as

$$\bar{U}_a^t = \hat{r}_a^t \hat{\lambda}_a^t + \sqrt{\frac{c' \ln t}{C_a^t}}. \quad (25)$$

We express the actual expected jammer interference $\hat{\lambda}_a^t$ as

$$\hat{\lambda}_a^t = \frac{\sum_{i=1}^{C_a^t} \lambda_{a,i}^t}{C_a^t}, \quad (26)$$

where $\sum_{i=1}^{C_a^t} \lambda_{a,i}^t$ represents the number of times the CIoT agent has experienced a jamming attack as a result of action a . Therefore, $\hat{\lambda}_a^t$ is a value between 0 and 1. Thus, for our proposed UCB-IA algorithm the adjusted Q-value is given by

$$\bar{Q}^\pi(s, a) = Q^\pi(s, a) + \bar{U}_a^t. \quad (27)$$

The adjustment of the Q-value using UCB-IA is illustrated in Fig. 2. This modification is applied to the Q-value output of the DDQN architecture, refining the action selection policy in accordance with the proposed UCB-IA strategy.

VI. Simulation Model and Results

In this section, we assess the effectiveness of our proposed DRL strategy featuring UCB-IA exploration in enhancing the transmission efficiency of the EH-enabled CIoT network detailed in Section II.

A. Simulation Settings

The CIoT Tx under study possesses the capability to dynamically select a transmit power P_s from the set $P = \{0.01, 0.02, \dots, 0.1\}$ based on the current environment state. Moreover, the CIoT Tx is equipped with a finite-sized battery whose initial level is $B_0 = 0$. We consider this scenario for the starting battery, since it is the worst-case scenario, offering a realistic view of the performance of our proposed DRL approach. The simulation parameters utilized can be found in Table II. The channel power gains g_{ss}^t and g_{sp}^t are distributed exponentially with mean values of 0.1 and 0.2, respectively. For simplicity, we assume $g_{sp}^t = g_{ps}^t$.

In the DDQN architecture, we employ four fully connected layers, each with a specific number of neurons: $j = 7$, $h_1 = 128$, $h_2 = 64$, and $z = 22$, without loss of generality. The leaky rectified linear unit (ReLU) serves as the non-linear activation function, with a leakiness parameter of $\alpha = 0.02$. The mean squared error (MSE) loss function \mathcal{L} in (22) is employed during training. As for the learning rate, we initialize it with $\eta = 4 \times 10^{-4}$, followed by a 50% reduction every 500 episodes. A penalty value of $\phi = 7$ is incurred whenever the CIoT agent violates the constraints outlined in (12) during the training phase. The training process consists of many episodes, each representing a time frame of T time slots. The proposed scheme was implemented on Google Colab using Python version 3.9.3 with a CPU hardware accelerator. Our reinforcement learning environment was developed using the Gymnasium library, and our deep learning models were built with the PyTorch 2.3.0 library.

In our evaluation, we employ performance metrics such as average sum rate (ASR), average reward, and jammer interference rate across training episodes. The total

Algorithm 1: The proposed UCB-IA-driven DRL Algorithm (12)

```

1 Input: Cognitive IoT environment simulator and
   its parameters.
2 Output: Optimal action  $a_t$  in each time slot  $t$ .
3 Initialize experience replay memory  $\mathcal{M}$  with size  $m$ .
4 Initialize battery level with  $B_0$ 
5 Initialize  $\forall \theta \in \Theta, \theta \sim \mathcal{N}(0, \frac{2}{v_i})$  and initialize  $\theta'$ 
   with  $\theta' \leftarrow \theta$ .
6 Initialize  $\eta$  and set the scheduler's reduction factor
   and patience period.
7 Initialize  $\gamma, \kappa$ , and  $c'$ .
8 for episode= 1,...,episodes do
9   for t= 1,...,T do
10    Observe the state  $s_t$ ;
11    if  $\mathcal{M}$  is not full then
12      Sample a random action  $a_t$ ;
13      Get the reward  $r_t$  using (15) and
         observe the next state  $s_{t+1}$  ;
14      Store  $\mathcal{M} \leftarrow (s_t, a_t, r_t, s_{t+1})$ ;
15    else
16      Calculate  $\bar{U}_a^t \leftarrow \hat{r}_a^t \hat{\lambda}_a^t + \sqrt{\frac{c' \ln t}{C_a^t}}$ ;
17      Adjust Q-value
18       $\bar{Q}^\pi(s, a) \leftarrow Q^\pi(s, a) + \bar{U}_a^t$ ;
19      Get action  $a_t$  according to the policy of
         adjusted Q-value;
20      Update action count,  $C_a^t \leftarrow C_a^t + 1$ ;
21      Get the reward  $r_t$  using (15) and
         observe the next state  $s_{t+1}$  ;
22      Update  $\hat{\lambda}_a^t \leftarrow (\sum_{i=1}^{C_a^t} \lambda_{a,i}^t) / C_a^t$ ;
23      Update  $\hat{r}_a^t \leftarrow (\sum_{i=1}^{C_a^t} r_{a,i}^t) / C_a^t$ 
24      Sample a mini-batch  $X$  from  $\mathcal{M}$  ;
25      Predict Target Q-values using (21);
26      Predict Q-values using  $Q^\pi(s, a; \theta)$ 
27      Calculate the loss in (22);
28      Update  $\theta$  of DDQN online using (24);
29      if episode*t mod  $\kappa = 0$  then
30        Update  $\theta'$  of Target DDQN online as
           $\theta' \leftarrow \theta$  ;
31      Update  $\eta$  using scheduler ;
32      Update  $\epsilon$  ;
33      Update the state  $s_{t+1} = s_t$ 

```

achievable sum rate of the CIoT Tx agent over T time slots (one episode) is expressed as $\sum_{t=1}^T R^t$, where R^t is defined in (11). The ASR is the weighted moving average of the total achievable sum rate. Furthermore, the total reward is calculated as all rewards accumulated by the CIoT Tx agent over one episode, given by $\sum_{t=1}^T r_t$, with r_t provided in (15). The average reward is the weighted moving average of the total reward of the CIoT agent. Finally, the jammer interference rate is determined by the number of time slots where the CIoT agent transmits data

TABLE II
Simulation Parameters

Parameters	Value
Number of time slots T	30
Duration of each time slot τ	1 s
Number of PU transmission slots L	18
Transmission power of PU P_p^t	0.2 W
Interference threshold I_{th}	0.01 W
Initial battery level B_0	0.0 W
Battery capacity B_{max}	0.5 W
Transmission power range of CIoT Tx P_s^t	0.01 ~ 0.1 W
Transmission power of jammer P_j^t	0.1 W
Maximum time slots under jamming ζ_{max}	12
Noise power σ^2	1e-3 W
Experience replay memory size m	10,000
Training episodes	2500
Mini-batch size	200
Learning rate η	4×10^{-4}
Learning rate reduction factor	50%
Learning rate patience period	500 episodes
Penalization ϕ	7
Discount factor γ	0.99
Leakiness parameter α	0.02
Update rate of Target DDQN κ	100
UCB adjustment term c'	1
Channel power gain of CIoT Tx-PU Rx g_{sp}^t	0.2 W
Channel power gain of CIoT Tx-Rx g_{ss}^t	0.1 W
Channel power gain of PU Tx-CIoT Rx g_{ps}^t	0.2 W
Number of neurons	7, 128, 64, 22

while the jammer is active, divided by the total number of time slots under jamming attacks. This rate is calculated as $\sum_{t=1}^T \lambda^t / \sum_{t=1}^T \omega_j^t$, where ω_j^t is defined in (4) and $\lambda^t = 1$ indicates that the CIoT agent experienced jamming in time slot t (with $\lambda^t = 0$ otherwise).

The calculation of the weighted moving average is as follows

$$\text{average}_{\text{new}} = (1 - \delta) \times \text{average}_{\text{old}} + \delta \times \text{value}, \quad (28)$$

where δ represents the significance according to the newest data point, with $1 - \delta$ reflecting the importance of the accumulated historical average. In this context, we have chosen $\delta = 0.01$. By utilizing the weighted moving average, short-term fluctuations are smoothed out, allowing the underlying trends in both sum rate and rewards to become more apparent. This method effectively balances the incorporation of recent data with the relevance of past information, thus refining our analysis of training episodes.

To assess the effectiveness of our proposed DRL approach, we compare the system performance with the following:

- The ϵ -greedy strategy, which is widely adopted in the literature to balance exploration and exploitation. Using the ϵ -greedy strategy, the CIoT agent selects an action aiming to maximize the estimated Q-value (exploitation) with a probability of $1 - \epsilon$, while opting for a random action (exploration) with a probability of ϵ .
- The Fixed strategy involves the CIoT agent determining its action a_t at each time step based on a rule-based approach derived from the constraints outlined

in (12), without employing any learning mechanisms [4].

- The Random strategy entails the CIoT agent selecting an action a_t at each time step randomly from the action space, without any cognitive or intelligent decision-making involved.

B. Simulation Results

To fairly compare our UCB-IA strategy with the ϵ -greedy strategy, Fig. 3 illustrates how different ϵ values affect the DRL algorithm's performance, allowing us to select the ϵ value that enhances the average sum rate (ASR). As the value of ϵ changes, the ASR of the CIoT agent changes considerably. When $\epsilon = 0.1$, the highest ASR is observed. This suggests that lower ϵ values strike an optimal balance between exploration and exploitation, enabling the CIoT agent to make informed decisions based on its acquired knowledge while intermittently exploring new actions. Conversely, as ϵ increases, a decline in the CIoT Tx's ASR becomes evident. The lowest performance occurs at $\epsilon = 0.9$, signifying that the CIoT agent heavily favors exploration and almost acts as the random strategy. This extensive exploration results in frequent penalties, as the CIoT agent randomly selects actions or disregards its learned knowledge, leading to suboptimal decisions and a decrease in overall performance. Therefore, we choose $\epsilon = 0.1$, which yields the best performance for the ϵ -greedy strategy to ensure a fair comparison with our proposed approach.

In Fig. 4, we present the ASR of the CIoT Tx across training episodes under several strategies. At the onset of training, both the proposed UCB-IA strategy and the ϵ -greedy strategy attain an ASR similar to the random strategy, since the CIoT agent is in the process of accumulating experiences in the replay memory. However, at convergence, it is evident that our proposed UCB-IA strategy attains the highest ASR when compared with all other strategies. The CIoT agent's high performance with our DRL approach comes from the UCB-IA algorithm. This algorithm modifies the Q-value, helping the CIoT agent balance the trade-off between exploitation and exploration, considering both expected reward and jammer interference. Consequently, this allows the CIoT network to effectively share the spectrum with the primary network while maximizing its throughput under malicious jamming.

The ϵ -greedy strategy outperforms the random and fixed strategies, yet it falls significantly short of our proposed UCB-IA strategy, proving it is not the optimum approach to balance the exploitation-exploration trade-off in such a dynamic CIoT environment. The random strategy exhibits the lowest ASR, as its random action selection diminishes the likelihood of successful data transmission. The fixed strategy, adhering to predefined rules, ranks second-lowest in ASR, highlighting suboptimal action choices due to the CIoT agent's inability to explore all potential actions that can improve the ASR.

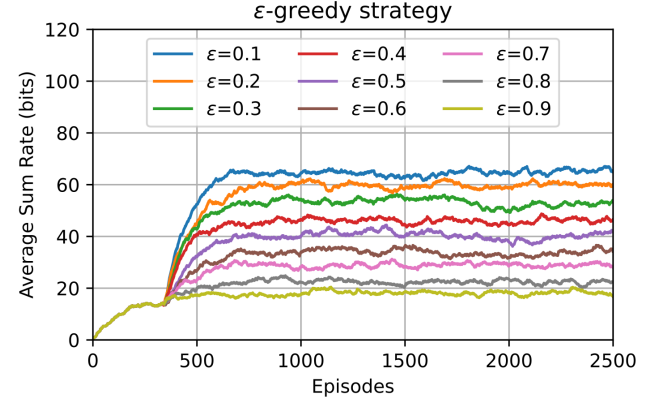


Fig. 3. The CIoT Tx's ASR performance with ϵ -greedy strategy across training episodes, comparison of different greediness value ϵ .

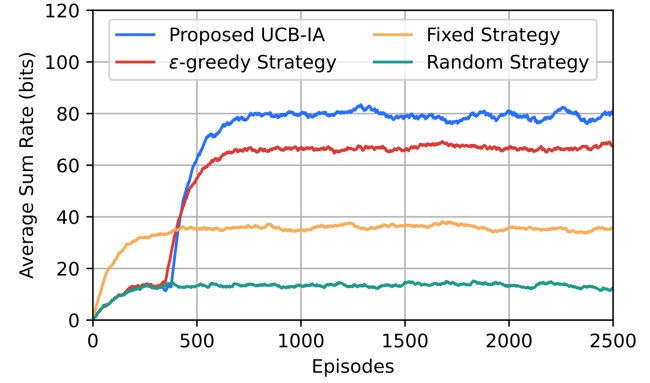


Fig. 4. The CIoT Tx's ASR performance across training episodes, comparison of different strategies.

Fig. 5 illustrates the average rewards obtained by the CIoT agent across training episodes using various strategies. The figure demonstrates the convergence of all the learning-based strategies, affirming the effectiveness of the training approach. For both the proposed UCB-IA and ϵ -greedy strategies, the reward remains zero at the beginning of training until the CIoT agent accumulates experiences in the replay buffer. Subsequently, both strategies exhibit a dip in rewards followed by an increase. This dip occurs because the DRL-based strategies favor long-term rewards over short-term rewards due to exploration. Similar to the trends observed in Fig. 4, our proposed DRL algorithm that employs the UCB-IA strategy attains the highest average reward, followed by the ϵ -greedy strategy and the fixed strategy, while the random strategy records the lowest reward.

The fixed strategy consistently yields positive rewards throughout all training episodes due to its adherence to hard-coded rules, preventing actions that result in penalties. Conversely, the random strategy yields negative rewards in all episodes, attributed to its random action selection. Comparing Fig. 4 and Fig. 5, it can be noticed that for both UCB-IA and ϵ -greedy, the ASR values

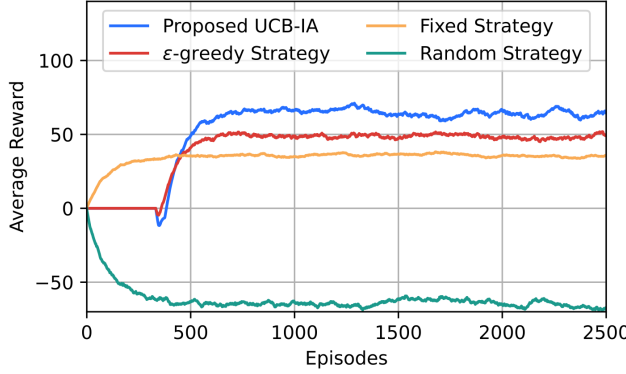


Fig. 5. The CIoT Tx's average achievable reward across training episodes under different strategies.

are higher than the corresponding reward values. This is because the average reward metric accounts for penalties incurred during the exploration of new actions. However, despite receiving penalties for exploration, the reward of our proposed UCB-IA strategy remains higher than that of the ϵ -greedy strategy.

In Fig. 6, we depict the jammer interference rate across all training episodes for the four previously discussed strategies. Observations reveal that the random strategy exhibits the highest interference rate $\sim 50\%$. This suggests that, on average, the CIoT agent chooses to transmit data during approximately half of the time slots when jamming signals are present, leading to penalties and data loss. Although the fixed strategy ensures a zero interference rate for the CIoT agent throughout all training episodes, its lower performance in achieving the ASR, as depicted in Fig. 4, suggests that it is not the optimal method. The zero interference rate achieved by the fixed strategy is due to its rule-based approach, which adheres to the constraints outlined in equation (12), particularly constraint (12d). This constraint dictates that the agent will switch to energy harvesting if the jammer is active during time slot t .

At the beginning of training, the jammer interference rate for the ϵ -greedy and the UCB-IA strategy follows an increasing trend as the CIoT agent is in the process of accumulating experiences. However, as training progresses, the CIoT agent using the ϵ -greedy strategy learns the actions that maximize the ASR, yet those actions ultimately result in an interference of 5% with the jammer at convergence. In contrast, when the CIoT agent uses the proposed UCB-IA strategy, it effectively learns actions that not only maximize the long-term throughput but also result in a 0% interference rate with the jammer. This implies that the UCB-IA strategy helps the CIoT device proficiently manage jammer interference on the same channel. It does so by harvesting from these interference signals, leading to higher battery levels and improved transmission success in future time slots.

In Fig. 7, we present the ASR for the four strategies

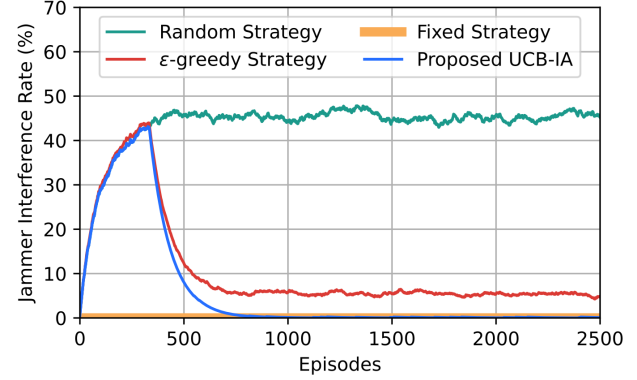


Fig. 6. The jammer interference rate with the CIoT agent across training episodes under different strategies.

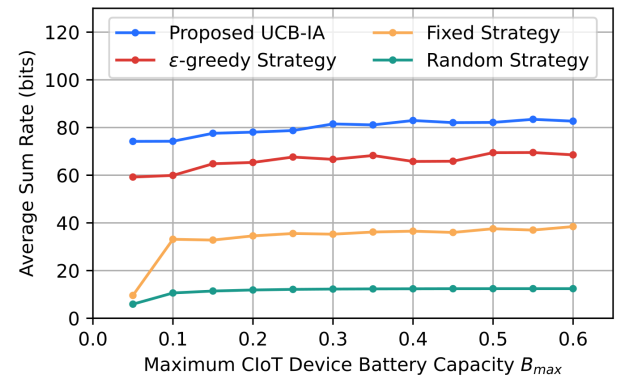


Fig. 7. The effect of the maximum battery capacity B_{max} of the CIoT agent on the ASR across different strategies.

across various values for maximum battery capacity B_{max} of the CIoT device. As depicted in the figure, increasing B_{max} allows the CIoT device to gather more energy through energy harvesting, resulting in increased ASR. Moreover, the increased capacity decreases the likelihood of battery overflow (when energy harvested exceeds B_{max}), thereby lowering the penalties faced by the CIoT agent. However, after reaching a certain threshold, any further increase in battery size offers minimal improvements, signifying a point of resource saturation.

At this stage, extra capacity fails to correspond to further performance enhancement. However, our proposed DRL algorithm that utilizes the UCB-IA strategy consistently outperforms all strategies across various values of B_{max} . This underscores the flexibility of our approach to optimize the ASR not only in scenarios with ample battery capacity but also in situations with limited capacity. It is important to highlight that, even at larger battery capacities, the performance of the CIoT agent employing the ϵ -greedy strategy still remains inferior to our proposed approach.

In Fig. 8, we present the ASR of the CIoT agent that uses our proposed DRL algorithm combined with the

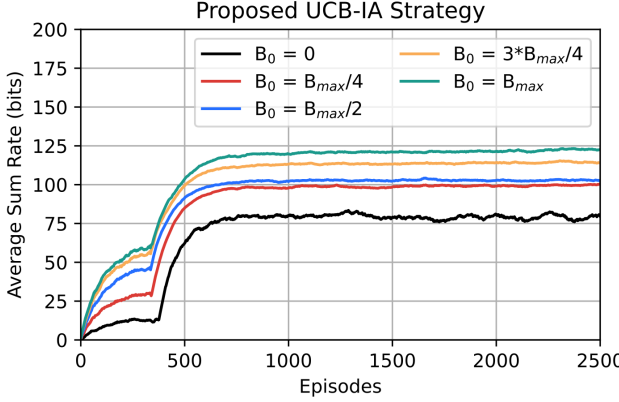


Fig. 8. The effect of starting battery level B_0 on the ASR of the CIoT Tx using our proposed UCB-IA approach.

UCB-IA strategy across all training episodes, considering various initial battery levels B_0 . Notably, the full battery configuration demonstrates the highest ASR compared to all other initial battery levels, while the empty battery configuration exhibits the lowest ASR. This is because, starting training with an empty battery limits the CIoT agent's available actions to achieve rewards, increasing the probability of choosing actions that result in penalties. Consequently, in such a scenario, the CIoT agent prioritizes energy harvesting in the early time slots to ensure the ability to transmit in subsequent time slots. Conversely, starting with a full battery allows the CIoT agent to prioritize data transmission, leading to higher rewards.

In Fig. 9, we present the ASR of the CIoT agent under various spectrum-sharing scenarios by varying the number of slots occupied by the PU Tx L . Notably, as L increases, there is a clear decrease in the ASR of all strategies. This decline can be attributed to the increased limitation on action selection by the CIoT agent as more occupied slots are introduced. This is because, during an occupied slot, the CIoT agent is restricted by the interference threshold I_{th} , necessitating the selection of lower transmit power P_s^t to avoid penalties that result in a lower ASR.

Moreover, it can be noticed that all strategies attain comparable performance at high values of L , which can be attributed to the fact that the PU Tx occupies nearly all the slots. On the other hand, at low values of L , the CIoT agent has more flexibility in selecting its transmit power and, consequently, results in a higher ASR. Nevertheless, at various values of L , our proposed DRL algorithm utilizing the UCB-IA strategy consistently outperforms all other strategies. This shows that our proposed DRL approach can allow the CIoT network to achieve its goal of throughput maximization while efficiently coexisting with the PU Tx, even as channel occupancy changes.

In Fig. 10, we present the ASR of the CIoT agent across various numbers of time slots T under different strategies. It is evident that as the number of time slots increases, the ASR of all strategies increases. This is

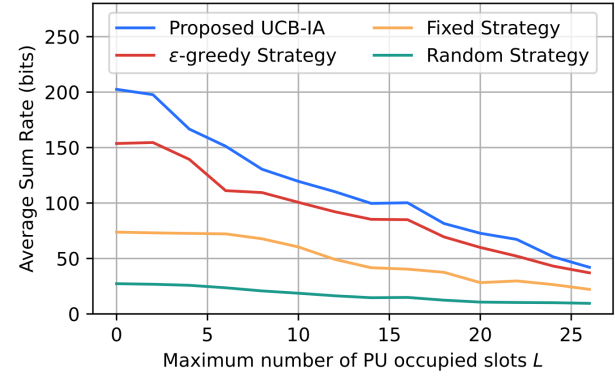


Fig. 9. The effect of the number of PU transmission slots L on the CIoT device's ASR across different strategies.

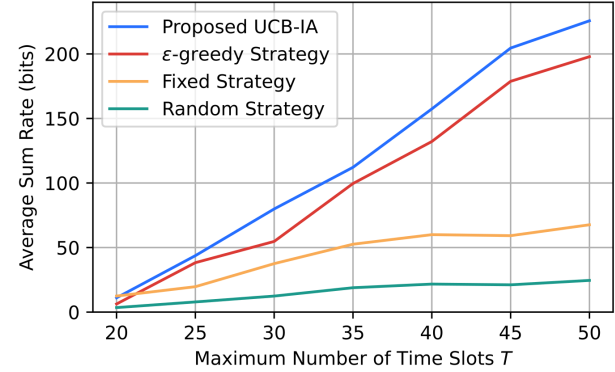


Fig. 10. The effect of the number of time slots T on the CIoT Tx's ASR across different strategies.

because, with a constant number of slots occupied by the PU Tx and targeted by the jammer, an increase in the number of time slots T offers the CIoT agent more chances for transmission without facing penalties. As depicted in the figure, the proposed UCB-IA strategy and the ϵ -greedy strategy demonstrate a more pronounced increase compared to the fixed and random strategies.

This significant contrast can be attributed to their learning nature, which enables them not only to select the optimal action at a given time slot but also to determine the most advantageous transmit power, directly influencing the ASR. At 20 time slots, the ASR values for all four strategies are nearly identical. This is because at $T = 20$ slots there are 18 slots occupied by the PU Tx and 10 slots subjected to jamming attacks. As a result, the available actions for the CIoT agent are restricted, resulting in all strategies converging on comparable choices. However, as T increases, the ASR of the proposed UCB-IA strategy and the ϵ -greedy strategy surpasses that of the fixed and random strategies by a considerable margin.

VII. Conclusions

In this paper, we introduced a novel DRL algorithm designed to help CIoT networks effectively manage the

exploitation-exploration trade-off in optimizing the action selection to achieve maximum ASR in malicious environments. This algorithm enables the CIoT agent to not only counteract jamming attacks but also utilize jamming interference to achieve its objectives and increase its lifetime. Our results show that the proposed DRL algorithm with the UCB-IA strategy meets its goals with considerable success, outperforming existing benchmarks significantly. This highlights the critical importance of tailoring DRL approaches to the specific system dynamics. We validated the algorithm's convergence under various network conditions, highlighting its potential to improve CIoT network performance even in challenging environments. These findings underscore the impact of learning algorithms in dynamic settings and suggest promising avenues for future research.

It is important to note that while our method excels in the specific context addressed in this paper, it may not always outperform existing benchmarks in simpler scenarios with fewer constraints. In such cases, our proposed strategy would achieve similar performance to existing benchmarks but would be less appealing due to its higher computational complexity and memory demands, making it more expensive to implement. Future research will focus on expanding the CIoT system model and investigating how network heterogeneity impacts performance. This expansion will require adjustments to the model and learning parameters, and the state and action spaces will become larger and more complex. To address these challenges and accelerate convergence, integrating transfer learning with DRL will be an interesting and promising direction for future work.

References

- [1] N. A. Khalek, D. H. Tashman, and W. Hamouda, "Advances in Machine Learning-Driven Cognitive Radio for Wireless Networks: A Survey," *IEEE Commun. Surveys Tuts.*, vol. 26, no. 2, pp. 1201–1237, 2024.
- [2] M. El Tanab and W. Hamouda, "Resource Allocation for Underlay Cognitive Radio Networks: A Survey," *IEEE Commun. Surveys Tuts.*, vol. 19, no. 2, pp. 1249–1276, 2017.
- [3] N. A. Khalek and W. Hamouda, "Intelligent Spectrum Sensing: An Unsupervised Learning Approach Based on Dimensionality Reduction," in *Proc. IEEE Int. Conf. Commun. (ICC)*, 2022, pp. 171–176.
- [4] N. A. Khalek, N. Abdolkhani, and W. Hamouda, "Deep Reinforcement Learning for Joint Power Control and Access Coordination in Energy Harvesting CIoT," *IEEE Internet Things J.*, 2024.
- [5] H. Han, Y. Xu, Z. Jin, W. Li, X. Chen, G. Fang, and Y. Xu, "Primary-User-Friendly Dynamic Spectrum Anti-Jamming Access: A GAN-Enhanced Deep Reinforcement Learning Approach," *IEEE Wireless Commun. Lett.*, vol. 11, no. 2, pp. 258–262, Feb. 2022.
- [6] H. Guo, Z. Yang, Y. Zou, M. Qian, J. Zhu, and L. Hanzo, "Joint Optimization of Power Splitting and Beamforming in Energy Harvesting Cooperative Networks," *IEEE Trans. Commun.*, vol. 67, no. 12, pp. 8247–8257, Dec. 2019.
- [7] X. Liu, M. Xia, P. Hu, K. Zheng, and S. Zhang, "Optimal Time Allocation for Energy Harvesting Cognitive Radio Networks with Multichannel Spectrum Sensing," *Wireless Commun. Mobile Comput.*, vol. 2022, p. 3940132, Aug. 2022.
- [8] O. O. Umeonwuka, B. S. Adejumobi, and T. Shongwe, "Deep Learning-Assisted Energy Prediction Modeling for Energy Harvesting in Wireless Cognitive Radio Devices," *IEEE Access*, vol. 12, pp. 8700–8720, 2024.
- [9] R. Lin, H. Qiu, J. Wang, Z. Zhang, L. Wu, and F. Shu, "Physical-Layer Security Enhancement in Energy-Harvesting-Based Cognitive Internet of Things: A GAN-Powered Deep Reinforcement Learning Approach," *IEEE Internet Things J.*, vol. 11, no. 3, pp. 4899–4913, 2024.
- [10] H. Pirayesh and H. Zeng, "Jamming Attacks and Anti-Jamming Strategies in Wireless Networks: A Comprehensive Survey," *IEEE Commun. Surveys Tuts.*, vol. 24, no. 2, pp. 767–809, 2022.
- [11] J. Xu, H. Lou, W. Zhang, and G. Sang, "An Intelligent Anti-Jamming Scheme for Cognitive Radio Based on Deep Reinforcement Learning," *IEEE Access*, vol. 8, pp. 202563–202572, 2020.
- [12] L. Jia, Y. Xu, Y. Sun, S. Feng, and A. Anpalagan, "Stackelberg Game Approaches for Anti-Jamming Defence in Wireless Networks," *IEEE Wireless Commun.*, vol. 25, no. 6, pp. 120–128, 2018.
- [13] A. Gousssem, K. Abualsaud, E. Yaacoub, T. Khattab, and M. Guizani, "Game Theory for Anti-Jamming Strategy in Multichannel Slow Fading IoT Networks," *IEEE Internet Things J.*, vol. 8, no. 23, pp. 16880–16893, 2021.
- [14] Y. Xu, Y. Xu, X. Dong, G. Ren, J. Chen, X. Wang, L. Jia, and L. Ruan, "Convert Harm Into Benefit: A Coordination-Learning Based Dynamic Spectrum Anti-Jamming Approach," *IEEE Trans. Veh. Technol.*, vol. 69, no. 11, pp. 13018–13032, 2020.
- [15] Y. Li, S. Bai, and Z. Gao, "A Multi-Domain Anti-Jamming Strategy Using Stackelberg Game in Wireless Relay Networks," *IEEE Access*, vol. 8, pp. 173609–173617, 2020.
- [16] I. K. Ahmed and A. O. Fapojuwo, "Stackelberg Equilibria of an Anti-Jamming Game in Cooperative Cognitive Radio Networks," *IEEE Trans. Cogn. Commun. Netw.*, vol. 4, no. 1, pp. 121–134, 2018.
- [17] X. Wang, J. Wang, Y. Xu, J. Chen, L. Jia, X. Liu, and Y. Yang, "Dynamic Spectrum Anti-Jamming Communications: Challenges and Opportunities," *IEEE Commun. Mag.*, vol. 58, no. 2, pp. 79–85, Feb. 2020.
- [18] A. S. Ali, S. Naser, and S. Muhamad, "Defeating Proactive Jammers Using Deep Reinforcement Learning for Resource-Constrained IoT Networks," in *Proc. IEEE Int. Symp. Pers. Indoor Mob. Radio Commun. (PIMRC)*, 2023, pp. 1–6.
- [19] W. Shen, W. Wang, H. Jin, and W. Zhang, "Defend Against Jamming Attacks Using Deep Reinforcement Learning," in *Proc. Int. Symp. Antennas Propag. EM Theory (ISAPE)*, Dec. 2021, pp. 1–3.
- [20] M. A. Aref and S. K. Jayaweera, "Robust Deep Reinforcement Learning for Interference Avoidance in Wideband Spectrum," in *Proc. IEEE Cogn. Commun. Aerosp. Appl. Workshop (CCAAW)*, Jun. 2019, pp. 1–5.
- [21] Q. Zhou, Y. Li, Y. Niu, Z. Qin, L. Zhao, and J. Wang, "One Plus One is Greater Than Two: Defeating Intelligent Dynamic Jamming with Collaborative Multi-agent Reinforcement Learning," in *Proc. IEEE Int. Conf. Comput. Commun. (ICCC)*, Dec. 2020, pp. 1522–1526.
- [22] Y. Bi, Y. Wu, and C. Hua, "Deep Reinforcement Learning Based Multi-User Anti-Jamming Strategy," in *Proc. IEEE Int. Conf. Commun. (ICC)*, May 2019, pp. 1–6.
- [23] M. A. Aref and S. K. Jayaweera, "Multi-task Deep Reinforcement Learning for Cognitive Spectrum-agile Communications," in *Proc. Conf. Ind. Inf. Syst. (ICIIIS)*, Dec. 2019, pp. 284–289.
- [24] Y. Li, Y. Xu, Y. Xu, X. Liu, X. Wang, W. Li, and A. Anpalagan, "Dynamic Spectrum Anti-Jamming in Broadband Communications: A Hierarchical Deep Reinforcement Learning Approach," *IEEE Wireless Commun. Lett.*, vol. 9, no. 10, pp. 1616–1619, Oct. 2020.
- [25] S. Liu, W. Li, L. Cui, X. Liu, X. Chen, R. Chen, Y. Li, and Y. Xu, "Flexible Channel Access Against Unknown Dynamic Jamming Attack: A Reinforcement Learning Approach," in *Proc. IEEE Int. Conf. Commun. China (ICCC)*, Aug. 2023, pp. 1–6.
- [26] S. Geng, P. Li, X. Yin, H. Lu, R. Zhu, W. Cao, and J. Nie, "The Study on Anti-Jamming Power Control Strategy based on Q-learning," in *Proc. Int. Conf. Intell. Comput. Signal Proc. (ICSP)*, 2022, pp. 182–185.
- [27] Y. Chen, Y. Li, D. Xu, and L. Xiao, "DQN-Based Power Control for IoT Transmission against Jamming," in *Proc. IEEE Veh. Technol. Conf. (VTC Spring)*, Jun. 2018, pp. 1–5.

- [28] P. K. H. Nguyen, V. H. Nguyen, and V. L. Do, "A Deep Double-Q Learning-based Scheme for Anti-Jamming Communications," in Proc. Eur. Signal Proc. Conf. (EUSIPCO), Jan. 2021, pp. 1566–1570.
- [29] A. S. Ali, W. T. Lunardi, L. Bariah, M. Baddeley, M. A. Lopez, J.-P. Giacalone, and S. Muhaidat, "Deep Reinforcement Learning Based Anti-Jamming Using Clear Channel Assessment Information in a Cognitive Radio Environment," in Proc. Int. Conf. Adv. Commun. Technol. Netw. (CommNet), Dec. 2022, pp. 1–6.
- [30] M. A. Aref and S. K. Jayaweera, "Spectrum-Agile Cognitive Radios Using Multi-Task Transfer Deep Reinforcement Learning," IEEE Trans. Wireless Commun., vol. 20, no. 10, pp. 6729–6742, Oct. 2021.
- [31] R. Lin, H. Qiu, W. Jiang, Z. Jiang, Z. Li, and J. Wang, "Deep Reinforcement Learning for Physical Layer Security Enhancement in Energy Harvesting Based Cognitive Radio Networks," Sensors, vol. 23, no. 2, 2023.
- [32] K. Ibrahim, S. X. Ng, I. M. Qureshi, A. N. Malik, and S. Muhaidat, "Anti-Jamming Game to Combat Intelligent Jamming for Cognitive Radio Networks," IEEE Access, vol. 9, pp. 137941–137956, 2021.
- [33] Q. Zhou, Y. Li, and Y. Niu, "A Countermeasure Against Random Pulse Jamming in Time Domain Based on Reinforcement Learning," IEEE Access, vol. 8, pp. 97164–97174, 2020.
- [34] Z. Shi, X. Xie, H. Lu, H. Yang, J. Cai, and Z. Ding, "Deep Reinforcement Learning-Based Multidimensional Resource Management for Energy Harvesting Cognitive NOMA Communications," IEEE Trans. Commun., vol. 70, no. 5, pp. 3110–3125, 2022.
- [35] M. Chu, X. Liao, H. Li, and S. Cui, "Power Control in Energy Harvesting Multiple Access System With Reinforcement Learning," IEEE Internet Things J., vol. 6, no. 5, pp. 9175–9186, 2019.
- [36] H. Xie, R. Lin, J. Wang, M. Zhang, and C. Cheng, "Power Allocation of Energy Harvesting Cognitive Radio Based on Deep Reinforcement Learning," in Proc. Int. Conf. Commun. Informat. Syst. (ICCIS), 2021, pp. 45–49.
- [37] R. S. Sutton and A. Barto, Reinforcement learning: An introduction. The MIT Press, 2020.
- [38] K. He, X. Zhang, S. Ren, and J. Sun, "Delving Deep into Rectifiers: Surpassing Human-Level Performance on ImageNet Classification," in Proc. IEEE Int. Conf. on Comput. Vis. (ICCV), 2015, pp. 1026–1034.
- [39] X. Chen, X. Xie, Z. Shi, and Z. Fan, "Dynamic Spectrum Access Scheme of Joint Power Control in Underlay Mode Based on Deep Reinforcement Learning," in Proc. IEEE Int. Conf. Commun. China (ICCC), 2020, pp. 536–541.
- [40] C. M. Bishop and N. M. Nasrabadi, Pattern recognition and machine learning. Springer, 2006, vol. 4, no. 4.
- [41] N. A. Khalek and W. Hamouda, "DeepSense: An Unsupervised Deep Clustering Approach for Cooperative Spectrum Sensing," in Proc. IEEE Int. Conf. Commun. (ICC), 2023, pp. 1868–1873.
- [42] N. A. Khalek, and W. Hamouda, "DEAP Learning: A Data-Driven Approach to Unsupervised Cooperative Spectrum Sensing," in Proc. IEEE Glob. Commun. Conf. (GLOBECOM), 2023, pp. 6389–6394.



Nadia Abdolkhani (Student Member, IEEE) received the B.Sc. and M.Sc. degrees in electrical engineering from Shiraz University of Technology, Shiraz, Iran, in 2017 and 2021, respectively. Currently, she is pursuing a Ph.D. from the Department of Electrical and Computer Engineering at Concordia University, Montreal, Canada. Her research interests include wireless and cellular communications, caching at wireless networks, device-to-device (D2D) communications, reinforcement learning-driven networks, and cognitive and cooperative communications.



Nada Abdel Khalek (Student Member, IEEE) received the M.Sc. degree in Electrical and Computer Engineering from Concordia University, Montreal, Quebec, Canada in 2020 and the B.Sc. degree (Magna Cum Laude) in Electronics and Communications Engineering from the American University in Cairo, Egypt, in 2018. She is currently pursuing her Ph.D. degree from the Department of Electrical and Computer Engineering at Concordia University. Her research focuses on intelligent

wireless communications, including deep learning and reinforcement learning-driven network operations, cognitive and cooperative communications, and spectrum sharing. She is a recipient of both Concordia University's International Tuition Award of Excellence and Merit Scholarship. Additionally, she received the Fonds de Recherche du Quebec - Nature and Technologies (FRQNT) Doctoral Fellowship for 2022 and the Best Paper Award from IEEE Globecom 2023.



Walaa Hamouda (Senior Member, IEEE) received the M.A.Sc. and Ph.D. degrees in electrical and computer engineering from Queen's University, Kingston, ON, Canada, in 1998 and 2002, respectively. Since July 2002, he has been with the Department of Electrical and Computer Engineering, Concordia University, Montreal, QC, Canada, where he is currently a Professor. Since June 2006, he is Concordia University Research Chair Tier I in Wireless Communications and Networking. His current research interests include machine-to-machine communications, IoT, 5G and beyond technologies, single/multiuser multiple-input multiple-output communications, space-time processing, cognitive radios, wireless networks. Dr. Hamouda served(ing) as Co-chair of the IoT and Sensor Networks Symposium of the GC'22, TPC Co-chair of the ITC/ADC 2022 conference, track Co-Chair: Antenna Systems, Propagation, and RF Design, IEEE Vehicular Technology Conference (VTC Fall'20), Tutorial Chair of IEEE Canadian Conference in Electrical and Computer Engineering (CCECE 2020), General Co-Chair, IEEE SmartNets 2019 Conference, Co-Chair of the MAC and Cross Layer Design Track of the IEEE (WCNC) 2019, Co-chair of the Wireless Communications Symposium of the IEEE ICC'18, Co-chair of the Ad-hoc, Sensor, and Mesh Networking Symposium of the IEEE GC'17, Technical Co-chair of the Fifth International Conference on Selected Topics in Mobile & Wireless Networking (MoWNet'2016), Track Co-Chair: Multiple Antenna and Cooperative Communications, IEEE Vehicular Technology Conference (VTC Fall'16), Co-Chair: ACM Performance Evaluation of Wireless Ad Hoc, Sensor, and Ubiquitous Networks (ACMPE-WASUN'14) 2014, Technical Co-chair of the Wireless Networks Symposium, 2012 Global Communications Conference, the Ad hoc, Sensor, and Mesh Networking Symposium of the 2010 ICC, and the 25th Queen's Biennial Symposium on Communications. He also served as the Track Co-chair of the Radio Access Techniques of the 2006 IEEE VTC Fall 2006 and the Transmission Techniques of the IEEE VTC-Fall 2012. From September 2005 to November 2008, he was the Chair of the IEEE Montreal Chapter in Communications and Information Theory. He is an IEEE ComSoc Distinguished Lecturer. He received numerous awards, including the Best Paper Awards of the IEEE GC 2023, IEEE GC 2020, IEEE ICC 2021, ICCSPA 2019, IEEE WCNC 2016, IEEE ICC 2009, and the IEEE Canada Certificate of Appreciation in 2007 and 2008. He served as an Associate Editor for the IEEE COMMUNICATIONS LETTERS, IEEE TRANSACTIONS ON SIGNAL PROCESSING, IEEE COMMUNICATIONS SURVEYS AND TUTORIALS, IET WIRELESS SENSOR SYSTEMS, IEEE WIRELESS COMMUNICATIONS LETTERS, TRANSACTIONS ON VEHICULAR TECHNOLOGY, and currently serves as an Editor for the IEEE TRANSACTIONS ON COMMUNICATIONS, IEEE TRANSACTIONS ON WIRELESS COMMUNICATIONS, IEEE IoT journal.